Article

Efficient Asymmetric Hydrogenation of Quinolines over Chiral Porous Polymers Integrated with Substrate Activation Sites

Lin Tao, Yiqi Ren, Chunzhi Li, He Li, Xuelian Chen, Lina Liu, and Qihua Yang

ACS Catal., **Just Accepted Manuscript** • DOI: 10.1021/acscatal.9b04838 • Publication Date (Web): 31 Dec 2019

Efficient Asymmetric Hydrogenation of Quinolines over Chiral Porous Polymers Integrated with Substrate Activation Sites

Lin Tao,[a,b] Yiqi Ren,[a,b] Chunzhi Li,[a,b] He Li,[a] Xuelian Chen,[c] Lina Liu, [a,b] and Qihua Yang[a,]*

[a]State Key Laboratory of Catalysis, *i*ChEM, Dalian Institute of Chemical Physics, Chinese Academy of Sciences, Dalian 116023, China.

[b]University of Chinese Academy of Sciences, Beijing 100049, China.

[c]Department of Chemistry, Laboratory of Advanced Materials, Fudan University, Shanghai 200433, China.

ABSTRACT. The heterogeneous asymmetric hydrogenation of quinolines for the production of optically active tetrahydroquinoline derivatives still remains a difficult task due to the aromatic stability of quinolines. Herein, we reported the efficient

heterogeneous asymmetric hydrogenation of quinolines over chiral porous polymers integrated with both chiral active sites (VDPEN-RuOTs) and substrate activation sites (TsOH). The porous polymer integrated with TsOH is 10 times more active than that without TsOH in the asymmetric hydrogenation of 2-methylquinoline. The volcano curve of TOF with TsOH/Ru ratio confirms the synergistic catalysis of VDPEN-RuOTs and TsOH. Comparison results with homogeneous catalytic system imply that the synergy between chiral centers and acid sites is greatly enhanced in the polymer network. Under optimized conditions, the chiral porous polymer afforded up to 90% ee with 90 h^{-1} TOF, which is one of the best solid catalysts for asymmetric hydrogenation of quinoline derivatives ever reported. Furthermore, the bi-functional porous polymers realized the asymmetric cascade hydrogenation/reductive amination reaction to obtain benzo-quinolizidines. Our primary results suggest that the incorporation of substrate activation sites near chiral centers is an efficient strategy for the synthesis of high-performance solid catalysts for heterogeneous asymmetric catalysis.

KEYWORDS: Heterogeneous asymmetric hydrogenation, quinolines, substrate activation, bi-functional polymer, synergistic effect.

1. INTRODUCTION

Asymmetric hydrogenation of quinolines with H_2 as hydrogen source is an atom-efficient and environmental benign approach for the synthesis of chiral 1,2,3,4-tetrahydroquinoline derivatives, which are important building blocks for the production of biological medicines.[1-3] Great progresses have been made in homogeneous asymmetric hydrogenation of quinolines since the first report by Zhou and co-workers in 2003.[4-6]

Heterogeneous asymmetric catalysis is very attractive in view of easy recycle of the expensive chiral catalysts, facile purification of products and possible continuous production of chiral compounds with fixed-bed reactors.[7-9] The heterogeneous asymmetric hydrogenation of quinolines was not fully investigated, despite of its importance. Fan and co-workers constructed Ru/Ir bimetallic dendronized polymer with (S)-BINAP and fluorene as building blocks as well as different generations of Fréchet-type dendritic DPEN ligands.[10] The dendronized polymer was used in the asymmetric hydrogenation of quinaldine, but the enantioselectivity was only about 70%. The (R)-BINAP conjugated microporous polymers reported by Liu and coworkers afforded 70% ee in the asymmetric hydrogenation of quinaldine after coordination with $[Ir(COD)Cl]_2$.[11] Recently, our group obtained up to 90% ee over polymer/CNTs composite (integrated with VDPEN-RuOTf) in the asymmetric hydrogenation of 2-methylquinoline.[12] But the catalytic activity is still not high enough in comparison with homogeneous counterpart. Up to date, it still

lacks of efficient and highly enantioselective solid catalysts for the asymmetric hydrogenation of quinoline derivatives.

One of the obstacles for the hydrogenation of quinoline derivatives is related with their aromatic stability which greatly increases the difficulty for the chemical transformation.[13, 14] To increase the reactivity of quinoline derivatives, substrate activation strategy has been previously reported with either chloroformate or Brönsted acids as activation reagents by Zhou[15] (with Ir-SegPhos as catalyst) and Fan[16] (with chiral cationic catalyst Cp*Ir(OTf)(MsDPEN) as catalyst). The activation reagents could destroy the aromaticity of quinoline derivatives to increase their reactivity and reduce the toxic effect of substrate on the catalyst.[14] However, the substrate activation strategy has not been reported in heterogeneous asymmetric catalytic system. Inspired by the success of the substrate activation strategy in homogeneous catalytic system, we aimed to synthesize bi-functionalized chiral solid catalysts possessing both chiral active sites and substrate activation sites for asymmetric hydrogenation of quinoline derivatives. In comparison with the direct addition of activation reagent during the catalysis, the bi-functional chiral solid catalysts have the advantages of facilitating the interactions among active sites, activation reagents and reactants, and avoiding the corrosion of equipment caused by acids.

Herein, porous polymer was chosen as a platform for the synthesis of bi-functional chiral solid catalysts considering its facile composition tunability.[17-19] The one-pot polymerization of (1R,2R)-N-(4-vinyl-benzenesulfonyl)-1,2-diphenylethane-1,2-diamine, sodium (4-vinylphenyl)methanesulfonate and 1,3,5-tri(4-vinylphenyl)benzene results in the formation of bi-functional chiral porous polymers with tunable ratio of chiral active sites to acid sites. The integration of acid sites in the polymer network dramatically increased the TOF from 8 h^{-1} to 90 h^{-1} in the asymmetric hydrogenation of 2-methylquinoline. Other than activity promotion, the

acid sites also improved the recycling stability of the solid catalyst. Furthermore, the potential of the bi-functional polymer catalysts was demonstrated in the synthesis of optically pure benzo-quinolizidines via the asymmetric cascade hydrogenation/reductive amination reaction.

2. EXPERIMENTAL SECTION

2.1. Chemicals and agents. Unless otherwise stated, all reagents were purchased from commercial sources and used without purification. Sodium (4-vinylphenyl)methanesulfonate (TsONa) and N,N-dimethylformamide (DMF) were purchased from Shanghai Chemical Reagent Company of the Chinese Medicine Group. p-Toluenesulfonic Acid was purchased from J&K Chemicals. Amberlyst-15 was purchased from Sigma-aldrich Company.

The cross-linking agent 1,3,5-tri(4-vinylphenyl)benzene (TVPB) was synthesized by Suzuki coupling of 1,3,5-tribromobenzene and 4-vinylphenylboronic acid on the basis of the literature method.[20] (1R,2R)-N-(4-vinylbenzenesulfonyl)-1,2-diphenylethane-1,2-diamine [(R,R)-VDPEN] and (1S,2S)-N-(4-vinylbenzenesulfonyl)-1,2-diphenylethane-1,2-diamine [(S,S)-VDPEN] were synthesized according to the literature method.[21, 22]

2.2. Synthesis of bi-functional porous polymers. Typically, desired amount of TVPB, (R,R)-VDPEN, TsONa and AIBN (5 wt% of monomers) were dissolved in DMF (200 mg monomers per mL) in a Schlenk tube and then heated at 80 ^{o}C for 20 h under N_2 atmosphere. The porous polymer was obtained by filtration followed by washing with DCM, water and methanol for several times and dried under vacuum at 80 ^{o}C for 5 h. The yield was about 90-95%. The TVPB/(VDPEN + TsONa) mole ratio of 1/1 was used in initial mixture for the synthesis of polymers. The polymer was denoted as P-C-A_X, where C and A respectively refer to chiral active sites and acid sites and $_X$ refers to the molar ratio of acid sites to chiral active sites. P-C(S)-A_X

was synthesized with a similar procedure to P-C-A_X except that (S,S)-VDPEN was used instead of (R,R)-VDPEN.

2.3. Transformation of porous polymers to bi-functional chiral catalysts. In a typical synthesis, 500 mg of P-C-A_X was added to 10 mL of dichloromethane containing 50 mg of $[Ru(p\text{-cymene})Cl_2]_2$ and the mixture was stirred at room temperature for 2 h. The solid material was filtrated and washed with sufficient amount of dichloromethane and methanol to remove the uncoordinated Ru salts, and the filtration was collected. The Ru concentration in the filtration was measured with UV-Vis spectrophotometer to calculate the Ru content in solid materials. After drying at room temperature under vacuum for 2 h, the solid material was dispersed in 10 mL of 0.6 M KOH solution and stirred vigorously at room temperature overnight. After filtration, washed copiously with water and dried under vacuum at 50 ^oC, the solid material was dispersed in 10 mL of methanol containing TsOH (10 equiv. corresponding to the amounts of chiral active sites in solid material) under N_2 atmosphere. After stirring the mixture for 2 h, the chiral catalyst P-C-A_X-RuOTs was obtained by filtration and washed with methanol under N_2 atmosphere.

A control sample, P-C-$A_{1.0}$-RuOTf, was prepared using a similar procedure to P-C-$A_{1.0}$-RuOTs with the exception that TfOH (5 equiv.) and CH_2Cl_2 (15 mL) were used in place of TsOH (10 equiv.) and methanol (10 mL), respectively.

2.4. General procedure for the asymmetric hydrogenation of quinoline derivatives. The asymmetric hydrogenation of quinoline derivatives was carried out in a 300 mL stainless steel autoclave equipped with a magnetic stirrer bar. The quinoline derivatives (0.74 mmol) and anhydrous methanol (1.0 ml) were added to a test tube containing desired amount of solid catalysts (7.4 μmol of Ru) in a glovebox. The test tube was transferred into the autoclave and the

autoclave was sealed. The H_2 pressure was adjusted to desired pressure after purging the autoclave with hydrogen for three times. The reaction mixture was stirred at required temperature for desired time interval. After reaction, the organic solution obtained by centrifugation was analyzed by gas chromatography with a HP-5 capillary column (30 m×0.32 mm×0.25 mm) to determine the conversion. After further purifying of the organic solution by flushing through a short pad of silica with petroleum ether and dichloromethane, the enantiomeric excess of the product was determined by HPLC with a chiral column OJ-H (for 2-methylquinline, 2-butylquinoline, 2,6-dimethyloquinoline) or OD-H (for 2-phenylquinoline, 6-fluoro-2-methylquinoline, 6-bromo-2-methylquinoline, 2-(4-methoxyl)phenylquinoline, 2-(2-naphthyl)quinoline).[23]

The recycling experiment was carried out in a glovebox under N_2 atmosphere. After each cycle, the catalyst was separated by centrifugation, washed with methanol (1 mL × 1) and n-hexane (1 mL × 3). Then another portion of substrate and solvent was added for the next cycle.

2.5. Asymmetric cascade hydrogenation/reductive amination reaction of 5-(quinolin-2-yl)pentan-2-one. 5-(Quinolin-2-yl)pentan-2-one (0.2 mmol) and anhydrous ethanol (1.0 mL) were added to a test tube containing desired amount of solid catalysts (4.0 μmol of Ru) in a glovebox. The test tube was transferred into a 300 mL stainless steel autoclave and the autoclave was sealed. The H_2 pressure was adjusted to 5 MPa after purging the autoclave with hydrogen for three times. The reaction mixture was stirred at 40 °C for 24 h. After reaction, the organic solution obtained by centrifugation was analyzed by ^{1}H NMR spectroscopy to determine the conversion and yield. After further purifying of the organic solution by flushing through a short pad of silica with petroleum ether and ethyl acetate (petroleum ether: ethyl acetate=10: 1), the enantiomeric excess and diastereomeric ratio of the product were determined by HPLC with the

connection of Chiralcel OD-H column and Chiralcel OJ-H column (hexane: isopropanol = 99: 1, flowing rate = 1.0 mL/min, 25 ^{o}C, UV detection at λ = 254 nm), t_{R1} = 10.2 min (major), t_{R2} = 14.4 min (minor).

2.6. Characterization. The nitrogen sorption isotherms were performed on an ASAP 2020 system at -196 ^{o}C after the samples were degassed at 120 ^{o}C for 5 h. The pore size distributions were calculated on the basis of the adsorption branch with a DFT model. The N and S elemental analysis was carried out separately on a HORIBA EMGA-930 Oxygen/Nitrogen/Hydrogen analyzer and a HORIBA EMIA-8100 Carbon/Sulfur analyzer. Transmission electron microscopy (TEM) was performed with a HITACHI 7700. The FT-IR spectra were recorded on a Nicolet IS50 IR spectrometer with KBr pellets. The UV-Vis spectra were performed on a SHIMADZU UV–Vis 2550 spectrophotometer. The ^{13}C CP-MAS NMR experiment was recorded on a Bruker DRX-400 with reference to tetramethylsilane. The solid-state CD spectra were recorded on a J-800 spectropolarimeter (Jasco, Japan). The Ru content in the solution for recycling experiment was determined by inductively coupled plasma atomic emission spectrometry (ICP-AES).

The acid exchange capacity of the catalysts was determined by acid–base titration with standard NaOH solution.[24] After drying under vacuum for 3 h, 50 mg of catalysts were dispersed in 40 mL of 2 M NaCl solution and the mixture was stirred vigorously for 24 h. Then the filtration was diluted to a constant volume and used for acid-base titration experiment.

3. RESULTS AND DISCUSSION

3.1. Synthesis and characterization of bi-functional chiral solid catalysts

In consideration of efficiency and facility to functionalize, we chose VDPEN-RuOTs (or VDPEN-RuOTf) as chiral active sites and TsOH as substrate activation sites for the synthesis of bi-functional porous polymer as illustrated in Scheme 1. The porous polymers P-C-A_X were

synthesized by radical polymerization method using 1,3,5-tri(4-vinylphenyl)benzene (TVPB), (1R,2R)-N-(4-vinyl-benzenesulfonyl)-1,2-diphenylethane-1,2-diamine [(R,R)-VDPEN] and sodium (4-vinylphenyl)methanesulfonate (TsONa) as monomers. TVPB was used as a crosslinker for the construction of porous polymer framework, while VDPEN and TsONa were respectively used as precursors for incorporation of chiral active sites and acidic sites. The chiral active sites to acidic sites ratio could be facilely tuned by varying the amounts of VDPEN and TsONa in the initial mixture. The catalyst P-C-A_X-RuOTs (or P-C-A_X-RuOTf) with VDPEN-RuOTs (or VDPEN-RuOTf) as chiral center and TsOH as activator was obtained via [Ru(p-cymene)Cl_2]$_2$ coordination followed by successive ion exchange as described in experimental section.[23]

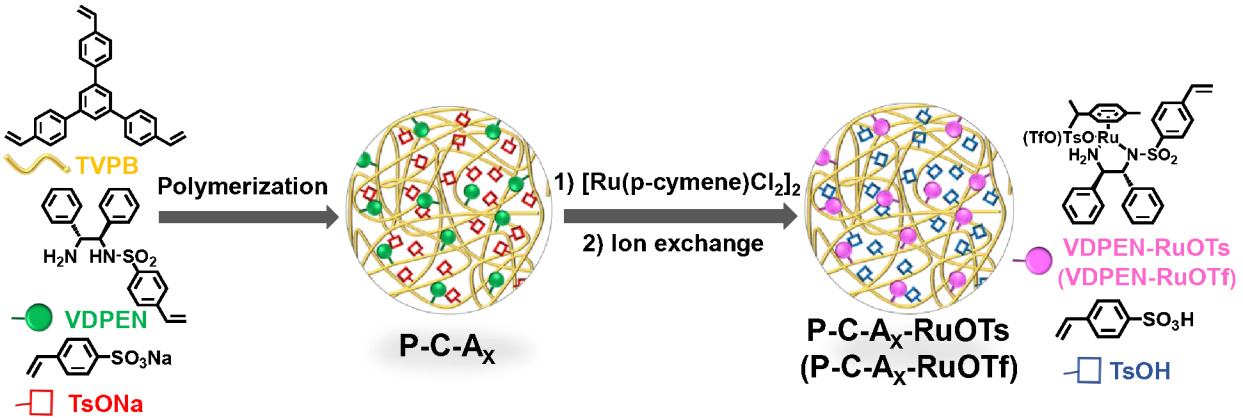

Scheme 1. Synthesis of bi-functional porous polymers via one-pot polymerization method and their transformation to bi-functional catalysts.

The textural properties of the bi-functional porous polymers were characterized by N_2 sorption analysis (Table 1, Figures 1, S1-S3). The N_2 sorption isotherms of all polymers gave sharp uptake at the relative pressure P/P_0 less than 0.1, showing the existence of micropore. The obvious H2 type hysteresis loop at relative pressure P/P_0 in the range of 0.4-0.9 showed that the polymers had mesopore. The bimodel pore size distribution curves confirmed the polymers had hierarchical micro/mesoporous structure (Figure S2). All the polymers had high BET surface

area in the range of 318-635 m^2/g and micropore of ~1.3 nm and mesopore of ~3.4 nm. As the content of TsONa monomer increasing, the BET surface area and pore volume increased. This is reasonable because the size of TsONa is smaller than that of VDPEN. The existence of disordered mesopore could be clearly observed in the TEM and HRTEM images of polymers, which is consistent with the results of N_2 sorption analysis (Figures 1, S3). The SEM image of representative P-C-$A_{1.0}$ illustrates that the polymer is composed of aggregated nanoparticles (Figure 1e).

Table 1. Physical and chemical parameters of P-C-A_X, P-C-A_X-RuOTs and P-C-$A_{1.0}$-RuOTf.

Sample	BET surface area (m^2/g)	Pore volume (cm^3/g)	Pore size (nm)	Ru (mmol/g)	Chiral ligand[a] (mmol/g)	SO_3Na[b] (mmol/g)	H^+[c] (mmol/g)
P-C-A_0	318	0.36	1.3, 3.4	-	1.43	-	-
P-C-A_0-RuOTs	352	0.65	1.6, 3.4	0.30	-	-	-
P-C-$A_{0.5}$	348	0.30	1.3, 3.4	-	0.98	0.15	-
P-C-$A_{0.5}$-RuOTs	413	0.41	1.7, 3.4	0.24	-	-	0.10
P-C-$A_{1.0}$	392	0.33	1.3, 3.4	-	0.71	0.48	-
P-C-$A_{1.0}$-RuOTs	551	0.60	1.3, 3.4	0.24	-	-	0.31
P-C-$A_{1.0}$-RuOTf	431	0.73	1.3, 3.4	0.24	-	-	0.36
P-C-$A_{2.0}$	635	0.52	1.2, 3.4	-	0.49	0.64	-
P-C-$A_{2.0}$-RuOTs	699	0.78	1.4, 3.4	0.21	-	-	0.53

[a] Calculated by 1/2mmol(N), where N content was measured by N elemental analysis. [b] Calculated by mmol(S)-1/2mmol(N), where S content was measured by S elemental analysis. [c] Determined by acid-base titration experiment.

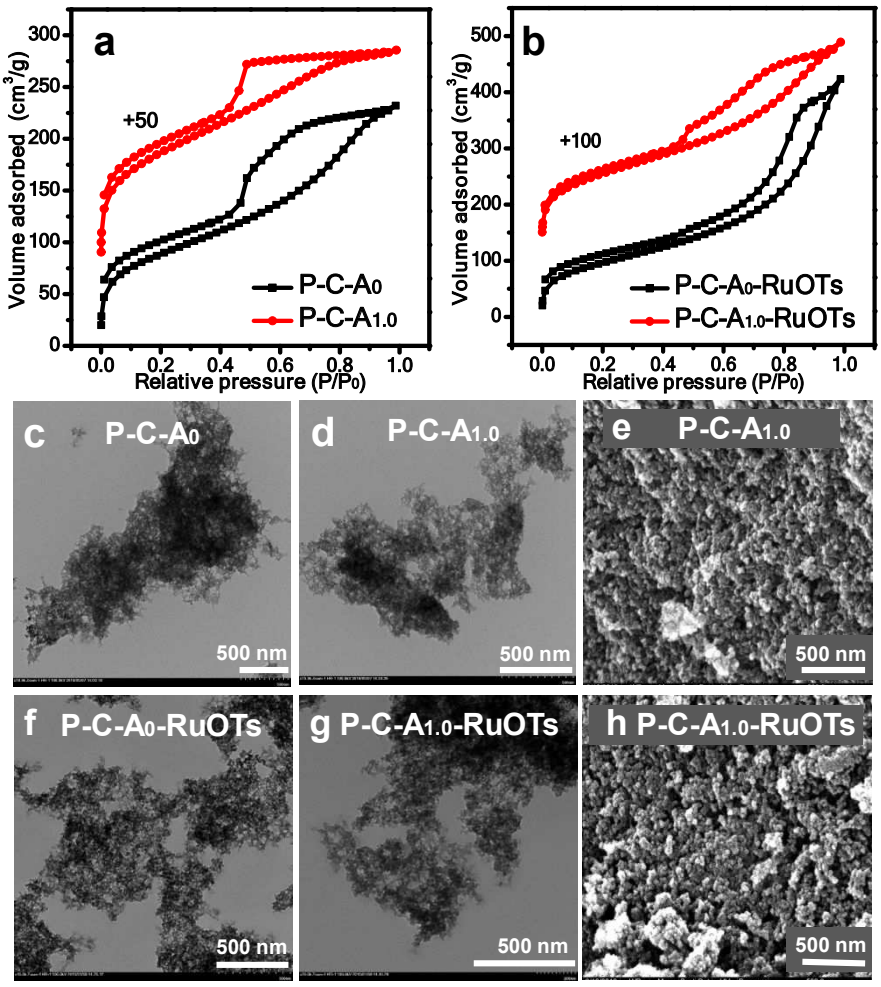

Figure 1. The N_2 sorption isotherms (a, b), TEM images (c, d, f, g) and SEM images (e, h) of porous polymers (a, c, d, e) before and after incorporation with Ru complex (b, f, g, h).

The bi-functional catalysts P-C-A_X-RuOTs had similar N_2 sorption isotherms to P-C-A_X with an exception that the H2 hysteresis loop at the relative pressure P/P_0 in the range of 0.4-0.9 became more obvious (Figures 1, S1). It is surprising that the BET surface area and pore volume of P-C-A_X-RuOTs increased significantly irrespective of the weight gain after Ru coordination. The variation in the textural parameters is related with the flexibility of porous polymer networks.[25] The TEM and SEM images of P-C-A_X-RuOTs were almost similar to those of P-C-

A_X, suggesting that the porous structure and morphology are well retained during the coordination and ion exchange process.

On the basis of elemental analysis, the contents of chiral ligand and -SO_3Na in P-C-A_X were calculated (Table 1). From P-C-A_0 to P-C-$A_{2.0}$, the content of –SO_3Na in the polymer increased from 0 to 0.64 mmol/g and the chiral ligand content decreased from 1.43 to 0.49 mmol/g. This demonstrates that the ratio of the two functional groups in the polymer could be facilely adjusted by simply varying the molar ratio of monomers in the initial mixture. To increase the usage efficiency of noble Ru, less than stoichiometric amount of $[Ru(p\text{-cymene})Cl_2]_2$ was used for the metal coordination. The Ru content of P-C-A_X-RuOTs was in the range of 0.21-0.30 mmol/g. The content of acid sites measured by acid–base titration experiment varied in the range of 0.10 to 0.53 mmol/g, suggesting the successful transformation of –SO_3Na to –SO_3H via ion-exchange method. The less H^+ than –SO_3Na indicates the incomplete transformation of –SO_3Na to –SO_3H, possibly due to the fact that some of –SO_3Na buried in the polymer network cannot be accessed during ion-exchange process. The control sample P-C-$A_{1.0}$-RuOTf had comparable physical and chemical parameters to P-C-$A_{1.0}$-RuOTs (Table 1, Figure S4).

P-C-A_X and P-C-A_X-RuOTs were further characterized by FT-IR spectroscopy (Figures 2a, 2b). The FT-IR spectra of P-C-A_X displayed characteristic vibrations of C-N at 1092 cm^{-1} and O=S=O at 1163 cm^{-1} and 1329 cm^{-1}, indicating the incorporation of VDPEN in the polymer network.[26] The FT-IR spectra of P-C-A_X-RuOTs were almost identical to those of P-C-A_X except that the relative peak intensity of characteristic band of O=S=O at 1163 cm^{-1} and 1329 cm^{-1} increased due to the formation of VDPEN-RuOTs. A new peak at 1258 cm^{-1} corresponding to the vibration of C-F bond was clearly observed in the FT-IR spectrum of P-C-$A_{1.0}$-RuOTf, confirming the successful formation of VDPEN-RuOTf (Figure S5).

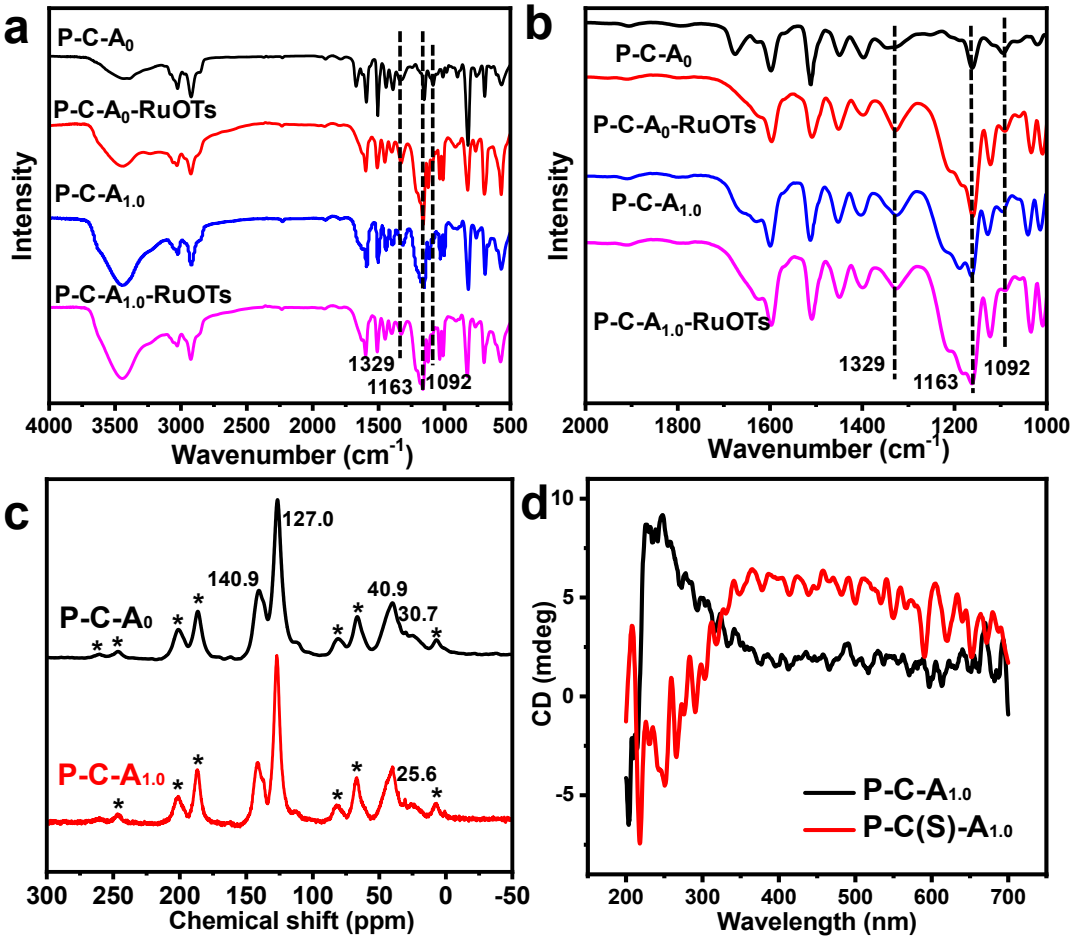

Figure 2. (a, b) The FT-IR spectra of P-C-A_X and P-C-A_X-RuOTs, (c) ^{13}C CP-MAS NMR spectra of P-C-A_0 and P-C-$A_{1.0}$, (d) CD spectra of P-C-$A_{1.0}$ and P-C(S)-$A_{1.0}$.

The ^{13}C CP-MAS NMR spectra of P-C-A_0 and P-C-$A_{1.0}$ clearly showed three sets of characteristic signals of carbon species (Figure 2c). The signals at 127.0 and 140.9 ppm could be assigned to the C of aromatic ring.[27] The peak at 40.9 ppm is assigned to the C connected with N in VDPEN. The signals at 30.7 and 25.6 ppm are attributed to the C of -CH_2-CH_2- formed after polymerization. The above results show that bi-functional porous polymers with tunable ratio of chiral active sites to acidic sites have been successfully synthesized by the one-pot polymerization method.

To identify the chirality of bi-functionalized porous polymer, (S,S)-VDPEN was also used as monomer to synthesize P-C(S)-$A_{1.0}$. The mirror solid state circular dichroism (CD) spectra of P-C-$A_{1.0}$ and P-C(S)-$A_{1.0}$ respectively displayed symmetric positive and negative signals originated from the (R,R)-VDPEN and (S,S)-VDPEN incorporated in the polymer network, suggesting that no racemization occurs for chiral ligands during the polymerization process (Figure 2d).

3.2. The promotion effect of acids in asymmetric hydrogenation of quinoline derivatives

2-Methylquinoline was chosen as a standard substrate for screening of the catalytic performance of bi-functional solid catalysts (Table 2). All P-C-A_X-RuOTs could catalyze the asymmetric hydrogenation reaction to afford ~90% ee. P-C-A_0-RuOTs only gave 67% yield of corresponding tetrahydroquinoline product in 12 h. The bi-functional P-C-A_X-RuOTs (x>0) catalysts afforded 99% yield under similar conditions. The TOF of P-C-A_X-RuOTs (x>0) is much higher than that of P-C-A_0-RuOTs, showing that the activity of porous polymer catalyst was significantly improved by incorporating TsOH in the polymer network. With H^+/Ru ratio increasing from 0.4 to 2.5, the TOF first increased from 39 to 90 h^{-1} and then decreased to 55 h^{-1} (Table 2, Figure 3a). The volcano curve of TOF with H^+/Ru ratio indicates the synergistic effect among chiral active sites and acidic sites. P-C-$A_{1.0}$-RuOTs with optimized H^+/Ru ratio afforded TOF approaching that of homogeneous counterpart (90 h^{-1} versus 132 h^{-1}). The control sample P-C-$A_{1.0}$-RuOTf with a TOF of 90 h^{-1} and 90% ee had similar activity to that of P-C-$A_{1.0}$-RuOTs. But for homogeneous catalysis, the activity of VDPEN-RuOTf is much higher than that of VDPEN-RuOTs. This might come from the different microenvironments of chiral active sites in homogeneous and heterogeneous catalysts. In the porous polymer, the TsO^- surrounding the chiral active sites might replace TfO^-, which causes the similar activity of P-C-$A_{1.0}$-RuOTf and P-C-$A_{1.0}$-RuOTs.

Table 2. The asymmetric hydrogenation of 2-methylquinoline over heterogeneous and homogeneous catalysts.[a]

Catalyst	Temp. (°C)	Yield[b] (%)	Ee[c] (%)	TOF[d] (h^{-1})
P-C-A_0-RuOTs	40	67	90	8
P-C-$A_{0.5}$-RuOTs	40	99	90	39
P-C-$A_{1.0}$-RuOTs	40	99	90	90
P-C-$A_{2.0}$-RuOTs	40	99	89	55
P-C-$A_{1.0}$-RuOTs	60	99	89	115
P-C-$A_{1.0}$-RuOTs	80	99	88	148
P-C-$A_{1.0}$-RuOTf	40	99	90	90
P-C(S)-$A_{1.0}$-RuOTs	40	99	90	91
VDPEN-RuOTf	40	99	95	211
VDPEN-RuOTs	40	99	95	132

a. Reaction conditions: 0.74 mmol of 2-methylquinoline in 1 mL of MeOH, 1.0 mol% catalyst, 5 MPa H_2, 40 °C, 12 h. b. Determined by GC. c. Determined by HPLC analysis with a chiral OJ-H column. d. Turnover frequency was calculated with conversion less than 30%.

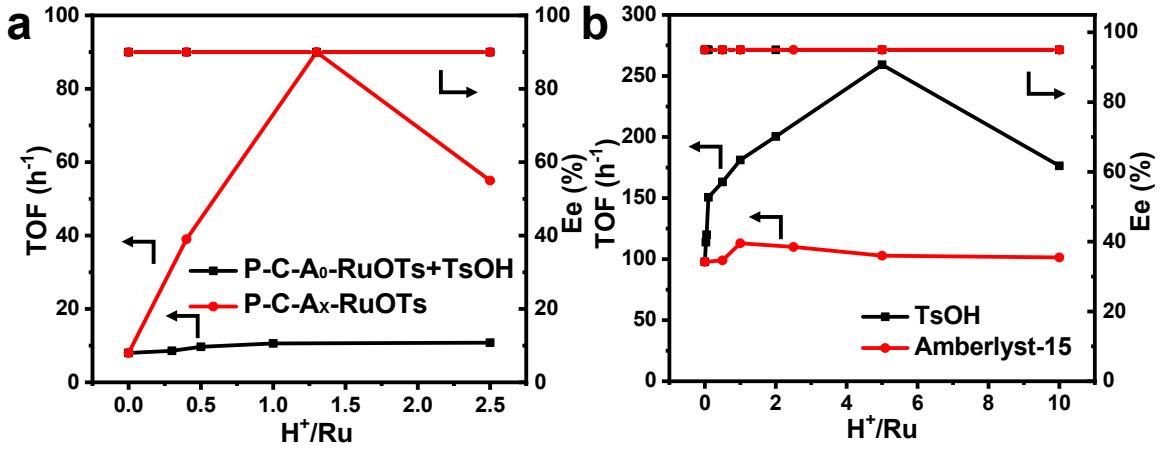

Figure 3. (a) The influence of H^+/Ru ratio on the TOF and ee of P-C-A_0-RuOTs and P-C-A_X-RuOTs, (b) the catalytic performance of VDPEN-RuOTs in the presence of TsOH and Amberlyst-15. Reaction conditions: S/C=100, 0.74 mmol of 2-methylquinoline, 1 mL methanol, 5 MPa H_2, 40 °C for (a) and room temperature for (b).

The control experiments were performed by addition of TsOH in the reaction system with P-C-A_0-RuOTs as catalyst. Unlike the bi-functional polymer, the TOF of P-C-A_0-RuOTs only increased slightly in the presence of TsOH (Figure 3a). The incorporation of ca. 1 equiv. acid sites in the polymer (P-C-$A_{1.0}$-RuOTs) could induce more than 10-fold increase in TOF, while the addition of ca. 1 equiv. TsOH in the catalytic system with P-C-A_0-RuOTs as catalyst only induced 1.3-fold increase in TOF. This suggests the synergy of chiral active sites and acidic sites is enhanced in the polymer network.

Another control experiment was performed by adding TsOH or Amberlyst-15 (sulfonated cross-linked polystyrene, concentration of acid sites is 4.7 mmol/g) in homogeneous catalytic system with VDPEN-RuOTs as catalyst (Figure 3b). The acceleration effect of TsOH was obviously observed. The TOF of VDPEN-RuOTs followed the volcano curve with H^+/Ru ratio and the highest TOF of 259 h^{-1} was obtained at H^+/Ru ratio of 5. Unexpectedly, the addition of Amberlyst-15 caused only slight increase in TOF. This is due to the low BET surface area of Amberlyst-15, which made the diffusion of VDPEN-RuOTs and substrate in its network difficult. It should be mentioned that the addition of TsOH or Amberlyst-15 caused no change in ee value. From the above results, we could draw a conclusion that the co-incorporation of chiral active sites and acidic sites in the polymer favors the synergistic effect during the catalytic process.

Higher reaction rate could be obtained at higher temperature (Table 2). For example, the TOF of P-C-$A_{1.0}$-RuOTs significantly increased to 115 h^{-1} and 148 h^{-1} at 60 ^oC and 80 ^oC. It should be mentioned that the ee value only decreased slightly and 88% ee could be obtained even at 80 ^oC. By comprehensive comparison of the activity and ee, P-C-$A_{1.0}$-RuOTs is one of the best solid catalysts ever reported for asymmetric hydrogenation of quinoline derivatives (Table S1).

Table 3. The asymmetric hydrogenation of quinoline derivatives with P-C-$A_{1.0}$-RuOTs as catalyst.[a]

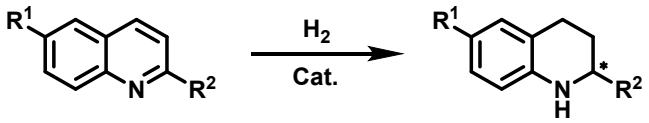

Entry	R^1	R^2	Temp. (^{o}C)	Yield[b] (%)	Ee[c] (%)
1	H	n-Bu	20	96	88
2	Me	Me	20	95	92
3	F	Me	20	94	90
4	Br	Me	20	96	88
5	H	Ph	40	87 (97)	72 (81)
6	H	4-methoxylphenyl	40	83 (95)	71 (80)
7[d]	H	2-naphthyl	40	99 (99)	50 (57)

a. Reaction conditions: S/C=100, 0.20 mmol substrate, 1 mL MeOH, 5 MPa H_2, 12 h. b. Determined by GC. c. Determined by HPLC analysis with a chiral OJ-H or OD-H column. The ee in brackets was obtained by VDPEN-RuOTs. d. 24 h, 2 mL MeOH.

With P-C-$A_{1.0}$-RuOTs as model catalyst, the substrate scope was screened (Table 3). Quinoline derivatives with electron donating or electron withdrawing substituent in the aromatic ring could be successfully converted into corresponding product over P-C-$A_{1.0}$-RuOTs with good to moderate ee. P-C-$A_{1.0}$-RuOTs afforded high activity and high ee for quinoline derivatives with Br, F, Me and n-Bu as substituents. It is worthwhile mentioning that 6-fluoro-2-methyltetrahydroquinoline, the important building block of flumequine, [28] could be obtained over P-C-$A_{1.0}$-RuOTs with 90% ee. P-C-$A_{1.0}$-RuOTs could also efficiently catalyze the asymmetric hydrogenation of substrates with more steric hindrance substituent such as aryl, 4-methoxylphenyl and 2-naphthyl, showing that the pore size of P-C-$A_{1.0}$-RuOTs is large enough for big molecules. P-C-$A_{1.0}$-RuOTs gave ee value of about 70% for 2-phenylquinoline and 2-(4-methoxyl)phenylquinoline. With 2-(2-naphthyl)quinoline as substrate, only 50% ee was obtained.

The low ee for substrates with more steric hindrance substituent over P-C-$A_{1.0}$-RuOTs is in a similar tendency to homogeneous counterpart. In summary, P-C-$A_{1.0}$-RuOTs has wide substrate scope.

3.3. Recycle stability of solid catalysts

The recycle stability of solid catalysts is of extreme importance for heterogeneous asymmetric catalysis. Our previous work showed that the leaching of anion (TfO^-) from the immobilized chiral center (VDPEN-RuOTf) occurred during the recycling process, which led to catalyst deactivation.[12] In this work, the bi-functional polymer is expected to strengthen the recycle stability considering the fact that the presence of acidic sites (TsOH) in the polymer network may compensate the leached anions. As shown in Figure 4a, P-C-$A_{1.0}$-RuOTs and P-C-$A_{1.0}$-RuOTf could be recycled five times without obvious loss of ee value. But slight decrease in activity could be observed during the recycling process. On the contrary, P-C-A_0-RuOTs showed sharp decrease in product yield and ee value at the second cycle (Figure 4b). The recycling results illustrate that the incorporation of TsOH in polymer network could not only promote the reactivity, but also help to improve the recycle stability of heterogeneous catalyst by providing a unique TsO^- enriched microenvironment surrounding the chiral center. The FT-IR spectra of reused P-C-$A_{1.0}$-RuOTf and P-C-$A_{1.0}$-RuOTs were almost identical to the corresponding fresh one with characteristic bands at 1163 cm^{-1} and 1329 cm^{-1} assigned to TsO^- (Figure 4c). The absence of characteristic vibration of C-F bond suggests the loss of TfO^- for the used P-C-$A_{1.0}$-RuOTf, which is consistent with our previous results.[12] Nevertheless, the recycle stability of P-C-$A_{1.0}$-RuOTf is improved, indicating that the leached TfO^- group from the VDPEN-RuOTf was supplemented by TsO^- integrated in the polymer network. The results again prove the superiority of the bi-functional catalyst.

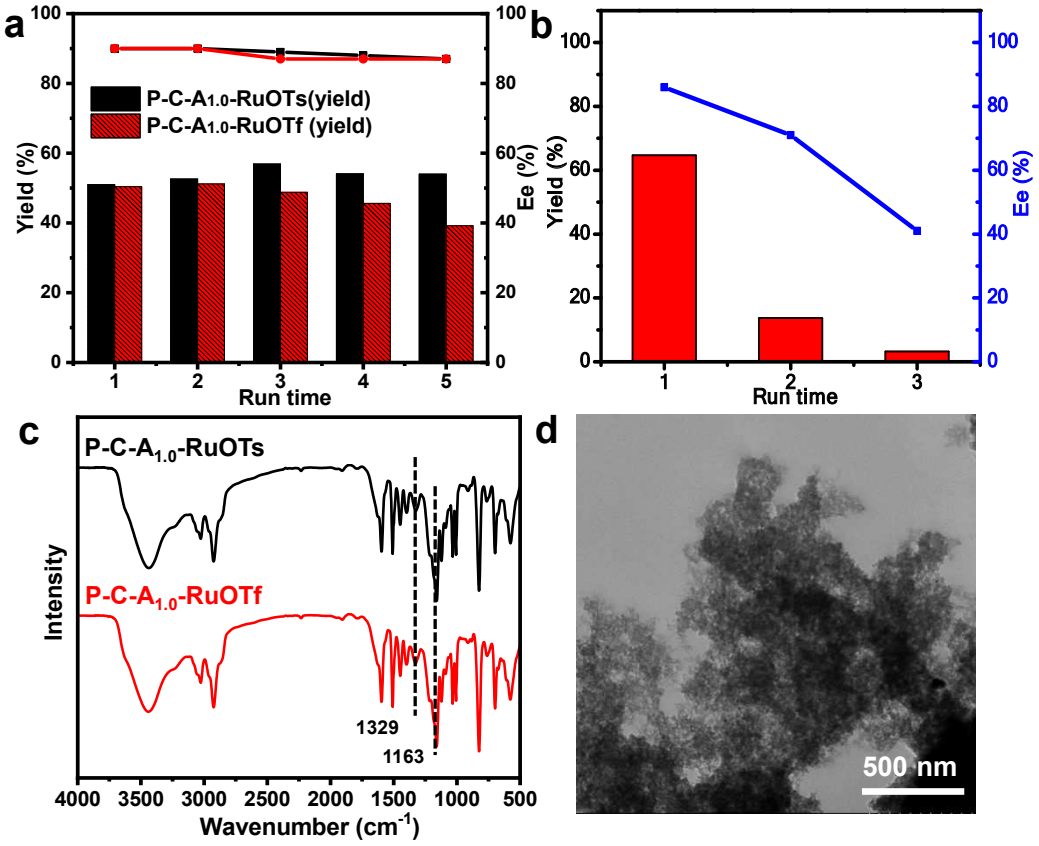

Figure 4. Recycling results of (a) P-C-$A_{1.0}$-RuOTs and P-C-$A_{1.0}$-RuOTf, (b) P-C-A_0-RuOTs in the asymmetric hydrogenation of 2-methylquinoline (reaction time for each cycle is extended by 20 min). (c) The FT-IR spectra of reused catalysts after five cycles. (d) TEM image of P-C-$A_{1.0}$-RuOTs after five cycles.

The porous structure of polymer catalyst was retained after recycling as evidenced by the almost identical TEM image of reused P-C-$A_{1.0}$-RuOTs to that of the fresh one (Figure 4d). In order to detect the leaching of Ru species, the filtrates of five cycles were collected and only 0.3% loss of Ru was found by ICP analysis. However, the acid amount of P-C-$A_{1.0}$-RuOTs and P-C-$A_{1.0}$-RuOTf after five cycles dropped down to 0.17 and 0.13 mmol/g, which explains the decrease in activity during recycling process. Further investigations to increase the stability of the solid catalysts are still needed.

3.4. Asymmetric cascade hydrogenation/reductive amination reaction for the synthesis of benzo-quinolizidines

The substituted chiral quinolizidines are important family of N-heterocycles and could be found in many natural alkaloids and pharmaceutical agents.[29, 30] The one-pot cascade catalytic asymmetric synthesis of chiral quinolizidines is a straightforward and economical way to obtain substituted chiral quinolizidines. Recently, Fan and coworkers firstly reported the direct synthesis of benzo-fused quinolizidines via cascade reaction with a combination of asymmetric hydrogenation of quinolines and intramolecular reductive amination using Ru/Ts-DPEN as chiral catalyst and TfOH as acid catalyst.[31]

Encouraged by Fan's work, we tested the catalytic performance of bi-functional porous polymers in synthesizing benzo-fused quinolizidines via cascade reaction with 5-(quinolin-2-yl)pentan-2-one as substrate (Table 4). Firstly, the catalytic performance of homogeneous catalyst VDPEN-RuOTs was tested. Without TsOH, VDPEN-RuOTs alone afforded 53% yield of target product with 90% ee, similar to previous report.[31] With the addition of 1 equiv. TsOH, the yield of target product increased to 68% without obvious change in both ee and dr. With the presence of 5 equiv. TsOH, up to 95% yield of the target product was obtained with 90% ee and dr of 19. This is consistent with the previous report that the presence of acid catalyst plays an important role in this cascade reaction.[31]

P-C-A_0-RuOTs only gave 25% yield of the target product, 70% ee and dr of 2, indicating that the polymer catalyst without acidic sites could not efficiently catalyze the cascade reaction. P-C-A_X-RuOTs (x>0) afforded much higher product yield, ee and dr than P-C-A_0-RuOTs. With the acid amount in the polymer increasing, the yield of quinolizidines increased gradually. P-C-$A_{0.5}$-RuOTs with H^+/Ru of 0.3 afforded product yield of 67%. P-C-$A_{1.0}$-RuOTs gave product yield of 75% with 90% ee and dr of 13. The yield increased up to 81% over P-C-$A_{2.0}$-RuOTs though slight decrease in ee and dr was observed. With similar H^+/Ru ratio, P-C-$A_{1.0}$-RuOTs is more

active than VDPEN-RuOTs (with 1 equiv. TsOH), suggesting that the close contact of the chiral active sites and acidic sites is very important for efficiently catalyzing the cascade reaction. In comparison with homogeneous counterpart, the obvious decrease in dr value for P-C-A_X-RuOTs may be due to the restricted movement of chiral active species integrated in the polymer network.

Table 4. The catalytic performance of homogeneous and heterogeneous catalyst in the asymmetric cascade hydrogenation/reductive amination of 5-(quinolin-2-yl)pentan-2-one.[a]

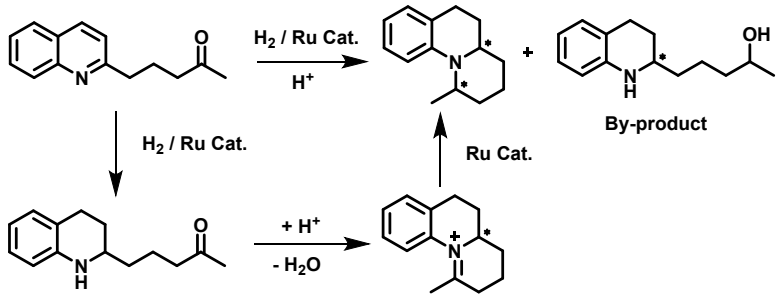

Catalyst	TsOH	Conv.[b] (%)	Yield[b] (%)	Dr[c]	Ee[c] (%)
VDPEN-RuOTs	-	99	53	21	90
VDPEN-RuOTs	1 equiv.	99	68	22	90
VDPEN-RuOTs	5 equiv.	99	>95	19	90
P-C-A_0-RuOTs	-	73	25	2	70
P-C-$A_{0.5}$-RuOTs	-	99	67	12	90
P-C-$A_{1.0}$-RuOTs	-	99	75	13	90
P-C-$A_{2.0}$-RuOTs	-	99	81	11	87

a. Reaction conditions: 0.2 mmol of substrate, 1 mL of EtOH, 2.0 mol % catalyst, 5 MPa H_2, 40 ^oC, 24 h. b. Determined by ^1H NMR. c. Determined by HPLC analysis with the connection of Chiralcel OD-H column and Chiralcel OJ-H column.

4. CONCLUSION

In summary, we have synthesized bi-functional porous polymer possessing both chiral centers (VDPEN-RuOTs) and substrate activation sites (TsOH) by one-pot polymerization method. The integration of TsOH in the polymer network greatly accelerated the reaction rate in asymmetric

hydrogenation of 2-methylquinoline, demonstrating the synergist effect of chiral centers and acid sites. With similar H^+/Ru ratio, the acceleration effect is more obvious for bi-functional solid catalyst in comparison with homogeneous counterpart, showing that the close contact of chiral centers and acid sites benefits the synergistic effect. Furthermore, incorporating TsOH in polymer network could also improve the recycle stability by providing a unique TsO^-enriched microenvironment surrounding the chiral center. Other than the asymmetric hydrogenation, the potential of the bi-functional polymer for catalyzing cascade asymmetric hydrogenation/reductive amination to construct benzo-quinolizidines has been demonstrated.

AUTHOR INFORMATION

Corresponding Author

* E-mail: yangqh@dicp.ac.cn,

Author Contributions

Lin Tao did all the experiments and wrote the manuscript, Yiqi Ren helped to synthesize the chiral monomer, Chunzhi Li and He Li discussed the data, Xuelian Chen gave help on SEM characterization, Lina Liu gave help on N_2 sorption experiment, Qihua Yang made the research plan, supervised the research and organized the manuscript. The manuscript was written through contributions of all authors.

Notes

The authors declare no competing financial interest.

ASSOCIATED CONTENT

Supporting Information. The TEM images, N_2 sorption isotherms, pore size distributions, HRTEM image, FT-IR spectrum of catalysts and the synthetic process of 5-(quinolin-2-yl)pentan-2-one could be found in supporting information. This material is available free of charge *via* the Internet at http://pubs.acs.org.

ACKNOWLEDGMENT

This work was financially supported by the Natural Science Foundation of China (No. 21733009, 21972134, 21621063) and the Strategic Priority Research Program of the Chinese Academy of Sciences Grant No. XDB17020200.

REFERENCES

1. Munoz, G. D.; Dudley, G. B. Synthesis of 1,2,3,4-Tetrahydroquinolines Including Angustureine and Congeneric Alkaloids. A Review. *Org. Prep. Proced. Int.* **2015,** *47*, 179-206.

2. DeKimpe, N.; Keppens, M. Novel Routes to Indoles, Indolines, Quinolines and Tetrahydroquinolines from N-(cyclohexylidene)amines. *Tetrahedron* **1996,** *52*, 3705-3718.

3. Sridharan, V.; Suryavanshi, P. A.; Menendez, J. C. Advances in the Chemistry of Tetrahydroquinolines. *Chem. Rev.* **2011,** *111*, 7157-7259.

4. Wang, W. B.; Lu, S. M.; Yang, P. Y.; Han, X. W.; Zhou, Y. G. Highly Enantioselective Iridium-catalyzed Hydrogenation of Heteroaromatic Compounds, Quinolines. *J. Am. Chem. Soc.* **2003,** *125*, 10536-10537.

5. Wang, D. S.; Chen, Q. A.; Lu, S. M.; Zhou, Y. G. Asymmetric Hydrogenation of Heteroarenes and Arenes. *Chem. Rev.* **2012,** *112*, 2557-2590.

6. He, Y. M.; Song, F. T.; Fan, Q. H. Advances in Transition Metal-Catalyzed Asymmetric Hydrogenation of Heteroaromatic Compounds. *Top Curr. Chem.* **2014,** *343*, 145-190.

7. Zhao, D. B.; Ding, K. L. Recent Advances in Asymmetric Catalysis in Flow. *ACS Catal.* **2013,** *3*, 928-944.

8. Fan, Q. H.; Li, Y. M.; Chan, A. S. C. Recoverable Catalysts for Asymmetric Organic Synthesis. *Chem. Rev.* **2002,** *102*, 3385-3465.

9. Heitbaum, M.; Glorius, F.; Escher, I. Asymmetric Heterogeneous Catalysis. *Angew. Chem. Int. Ed.* **2006,** *45*, 4732-4762.

10. Huang, Y. Y.; Yang, X.; Feng, Y.; Verpoort, F.; Fan, Q. H. Chiral Ru/Ir Bimetallic Dendronized Polymer Catalysts Constructed through Sequential Metal Coordination and Applied in Asymmetric Hydrogenation of Quinaldine. *J. Mol. Catal. A: Chem.* **2014,** *393*, 150-155.

11. Wang, X.; Li, J.; Lu, S. M.; Liu, Y.; Li, C. Efficient Enantioselective Hydrogenation of Quinolines Catalyzed by Conjugated Microporous Polymers with Embedded Chiral BINAP Ligand. *Chin. J. Catal.* **2015,** *36*, 1170-1174.

12. Tao, L.; Li, C. Z.; Ren, Y. Q.; Li, H.; Chen, J.; Yang, Q. H. Synthesis of Polymer/CNTs Composites for the Heterogeneous Asymmetric Hydrogenation of Quinolines. *Chin. J. Catal.*

2019, *40*, 1548-1556.

13. Balakrishna, B.; Nunez-Rico, J. L.; Vidal-Ferran, A. Substrate Activation in the Catalytic Asymmetric Hydrogenation of N-Heteroarenes. *Eur. J. Org. Chem.* **2015,** 5293-5303.

14. Yu, Z. K.; Jin, W. W.; Jiang, Q. B. Bronsted Acid Activation Strategy in Transition-Metal Catalyzed Asymmetric Hydrogenation of N-Unprotected Imines, Enamines, and N-Heteroaromatic Compounds. *Angew. Chem. Int. Ed.* **2012,** *51*, 6060-6072.

15. Wang, D. S.; Zhou, Y. G. Asymmetric Hydrogenation of Quinolines Activated by Bronsted Acids. *Tetrahedron Lett.* **2010,** *51*, 3014-3017.

16. Li, Z. W.; Wang, T. L.; He, Y. M.; Wang, Z. J.; Fan, Q. H.; Pan, J.; Xu, L. J. Air-Stable and Phosphine-Free Iridium Catalysts for Highly Enantioselective Hydrogenation of Quinoline Derivatives. *Org. Lett.* **2008,** *10*, 5265-5268.

17. Leadbeater, N. E.; Marco, M. Preparation of Polymer-Supported Ligands and Metal Complexes for Use in Catalysis. *Chem. Rev.* **2002,** *102*, 3217-3273.

18. Kramer, S.; Bennedsen, N. R.; Kegnaes, S. Porous Organic Polymers Containing Active Metal Centers as Catalysts for Synthetic Organic Chemistry. *ACS Catal.* **2018,** *8*, 6961-6982.

19. Sun, Q.; Dai, Z. F.; Meng, X. J.; Xiao, F. S. Porous Polymer Catalysts with Hierarchical Structures. *Chem. Soc. Rev.* **2015,** *44*, 6018-6034.

20. Gopalakrishnan, D.; Dichtel, W. R. Direct Detection of RDX Vapor Using a Conjugated Polymer Network. *J. Am. Chem. Soc.* **2013,** *135*, 8357-8362.

21. Sun, Q.; Jin, Y. Y.; Zhu, L. F.; Wang, L.; Meng, X. J.; Xiao, F. S. Superhydrophobic, Chiral, and Mesoporous TsDPEN Copolymer Coordinated to Ruthenium Species as an Efficient Catalyst for Asymmetric Transfer Hydrogenation. *Nano Today* **2013,** *8*, 342-350.

22. Zhang, X. M.; Zhao, Y. P.; Peng, J.; Yang, Q. H. Polymer@silica Composites with

Tunable Outer and Inner Surface Properties: A Platform for Aqueous Asymmetric Transfer Hydrogenation. *Green Chem.* **2015,** *17*, 1899-1906.

23. Wang, T. L.; Zhuo, L. G.; Li, Z. W.; Chen, F.; Ding, Z. Y.; He, Y. M.; Fan, Q. H.; Xiang, J. F.; Yu, Z. X.; Chan, A. S. C. Highly Enantioselective Hydrogenation of Quinolines Using Phosphine-Free Chiral Cationic Ruthenium Catalysts: Scope, Mechanism, and Origin of Enantioselectivity. *J. Am. Chem. Soc.* **2011,** *133*, 9878-9891.

24. Zhang, X. M.; Zhao, Y. P.; Xu, S. T.; Yang, Y.; Liu, J.; Wei, Y. X.; Yang, Q. H. Polystyrene Sulphonic Acid Resins with Enhanced Acid Strength via Macromolecular Self-assembly within Confined Nanospace. *Nat. Commun.* **2014,** *5,* 3170.

25. Zhong, M. M.; Li, H.; Chen, J.; Tao, L.; Li, C.; Yang, Q. H. Cooperative Activation of Cobalt-Salen Complexes for Epoxide Hydration Promoted on Flexible Porous Organic Frameworks. *Chem-Eur. J.* **2017,** *23*, 11504-11508.

26. Arakawa, Y.; Chiba, A.; Haraguchi, N.; Itsuno, S. Asymmetric Transfer Hydrogenation of Aromatic Ketones in Water using a Polymer-Supported Chiral Catalyst Containing a Hydrophilic Pendant Group. *Adv. Synth. Catal.* **2008,** *350*, 2295-2304.

27. Ohkuma, T.; Utsumi, N.; Tsutsumi, K.; Murata, K.; Sandoval, C.; Noyori, R. The Hydrogenation/Transfer Hydrogenation Network: Asymmetric Hydrogenation of Ketones with Chiral η^6-Arene/N-Tosylethylenediamine-Ruthenium(II) Catalysts. *J. Am. Chem. Soc.* **2006,** *128*, 8724-8725.

28. Yang, Z. S.; Chen, F.; He, Y. M.; Yang, N. F.; Fan, Q. H. Efficient Asymmetric Hydrogenation of Quinolines in Neat Water Catalyzed by Chiral Cationic Ru-Diamine Complexes. *Catal. Sci. Technol.* **2014,** *4*, 2887-2890.

29. Zhang, Q. Y.; Tu, G. Z.; Zhao, Y. Y.; Cheng, T. M. Novel Bioactive Isoquinoline

Alkaloids from Carduus Crispus. *Tetrahedron* **2002,** *58*, 6795-6798.

30. Winn, M.; Zaugg, H. E. Intramolecular Amidoalkylations at Carbon. Synthesis of Heterocyclic Amines. *J. Org. Chem.* **1968,** *33*, 3779-3783.

31. Chen, Y.; He, Y. M.; Zhang, S. S.; Miao, T. T.; Fan, Q. H. Rapid Construction of Structurally Diverse Quinolizidines, Indolizidines, and Their Analogues via Ruthenium-Catalyzed Asymmetric Cascade Hydrogenation/Reductive Amination. *Angew. Chem. Int. Ed.* **2019,** *58*, 3809-3813.